Neuron

Supplemental Information

Excitatory Cerebellar Nucleocortical Circuit Provides Internal Amplification during Associative Conditioning

Zhenyu Gao, Martina Proietti-Onori, Zhanmin Lin, Michiel M. ten Brinke, Henk-Jan Boele, Jan-Willem Potters, Tom J.H. Ruigrok, Freek E. Hoebeek, and Chris I. De Zeeuw

Supplemental Figures

Gao *et al*., Figure S1

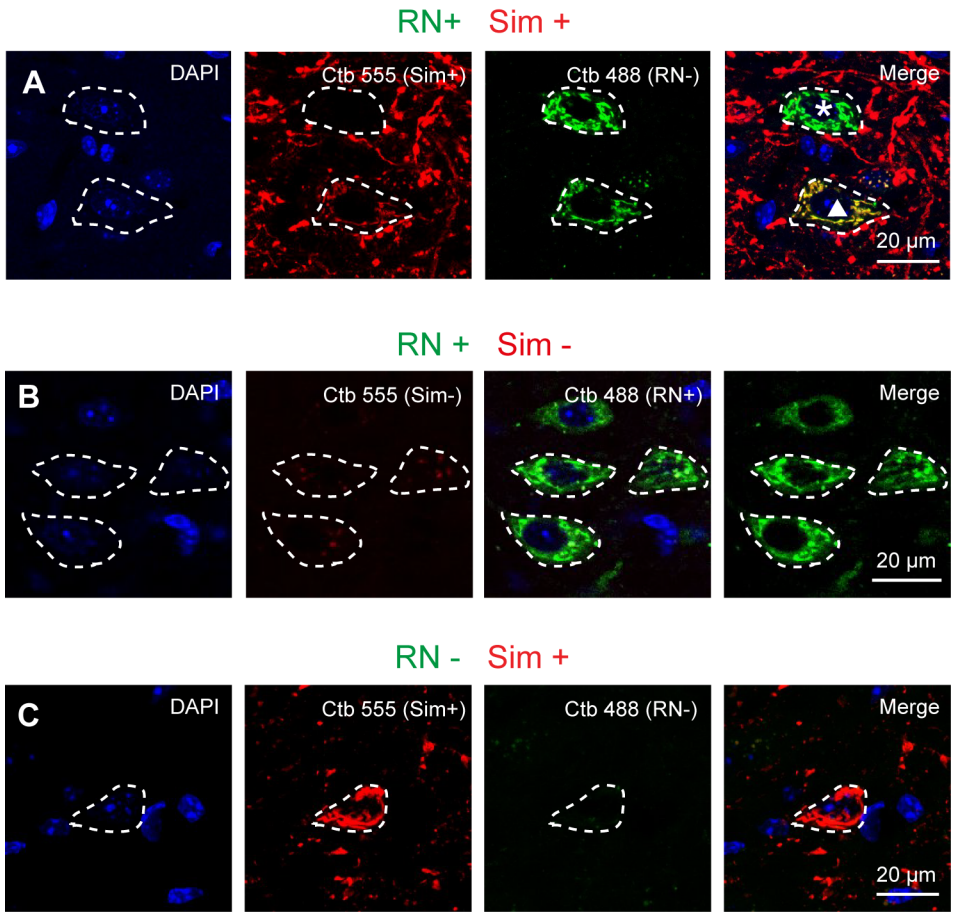

Figure S1. Related to Figure 1. Representative neurons in the IpN with retrograde labeling from red nucleus (RN, Ctb Alexa 488, green) and lobule simplex (Sim, Ctb Alexa 555, red)
(A) Confocal images showing co-labeled IpN neurons (triangle) and a neighboring neuron with RN labeling only (asterisk). (B) Confocal images showing IpN neurons with retrograde labeling from RN only. (C) Confocal images showing an IpN neuron with retrograde labeling from Sim only.

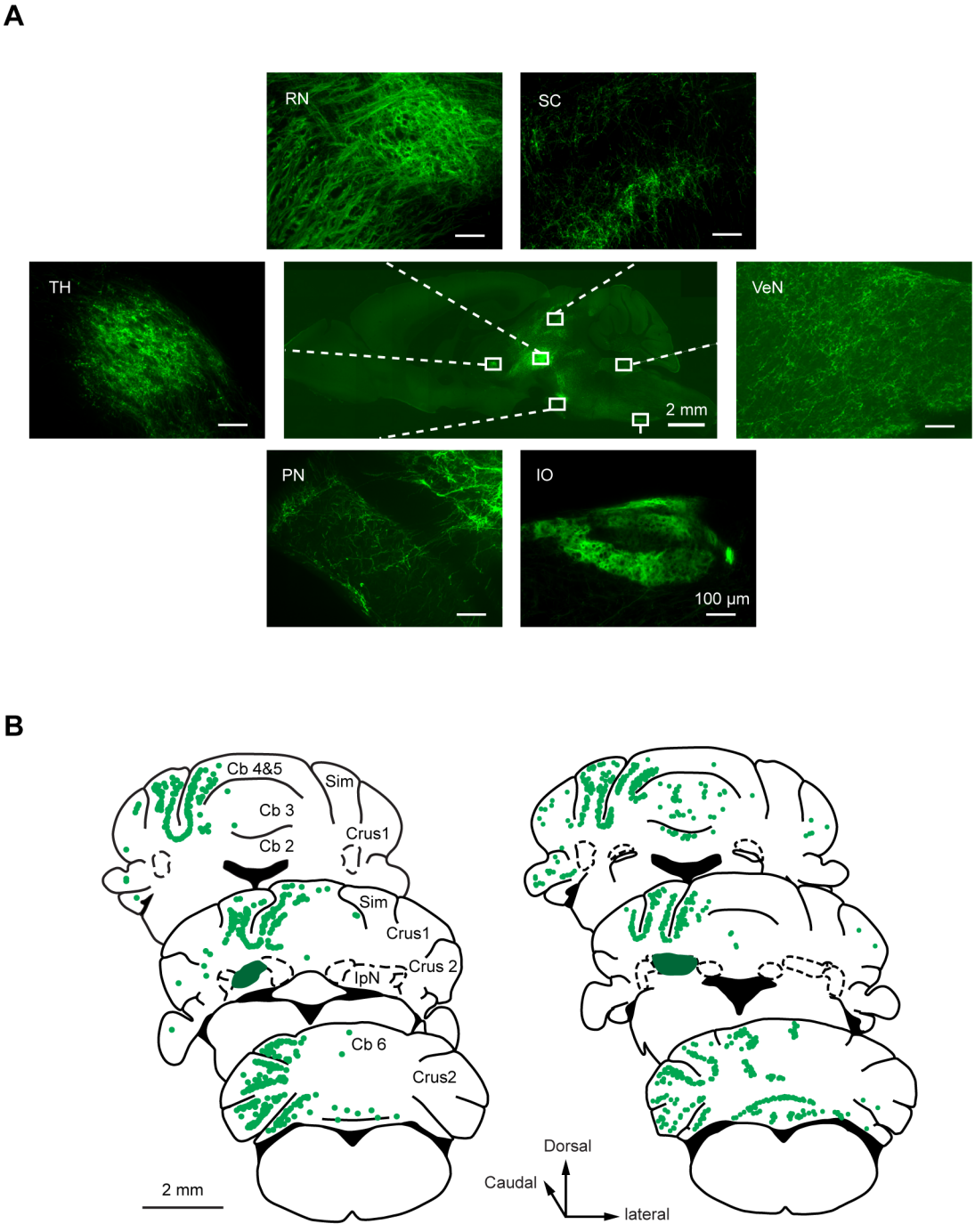

Figure S2. Related to Figure 1. eYFP labeled axonal projections in the IpN targeting regions
(A) Middle: Overview of axonal labeling throughout mouse brain in a sagittal section. Widespread axonal labeling can be found in the mouse in which 100 nl of AAV2-hSyn-hChR2(H134R)-eYFP was injected in the IpN nucleus. Surrounding: High magnification images indicating axonal labeling in the thalamus (TH), red nuclei (RN), superior colliculus (SC), vestibular nuclei (VeN), pontine nuclei (PN) and inferior olive (IO). (B) Representative distribution of nucleocortical MF rosettes in the cerebellar cortex. Schematics show coronal sections from two mice, throughout the regions in which dense nucleocortical MF labeling was observed. The initial IpN injection sites are indicated in dark green contours.

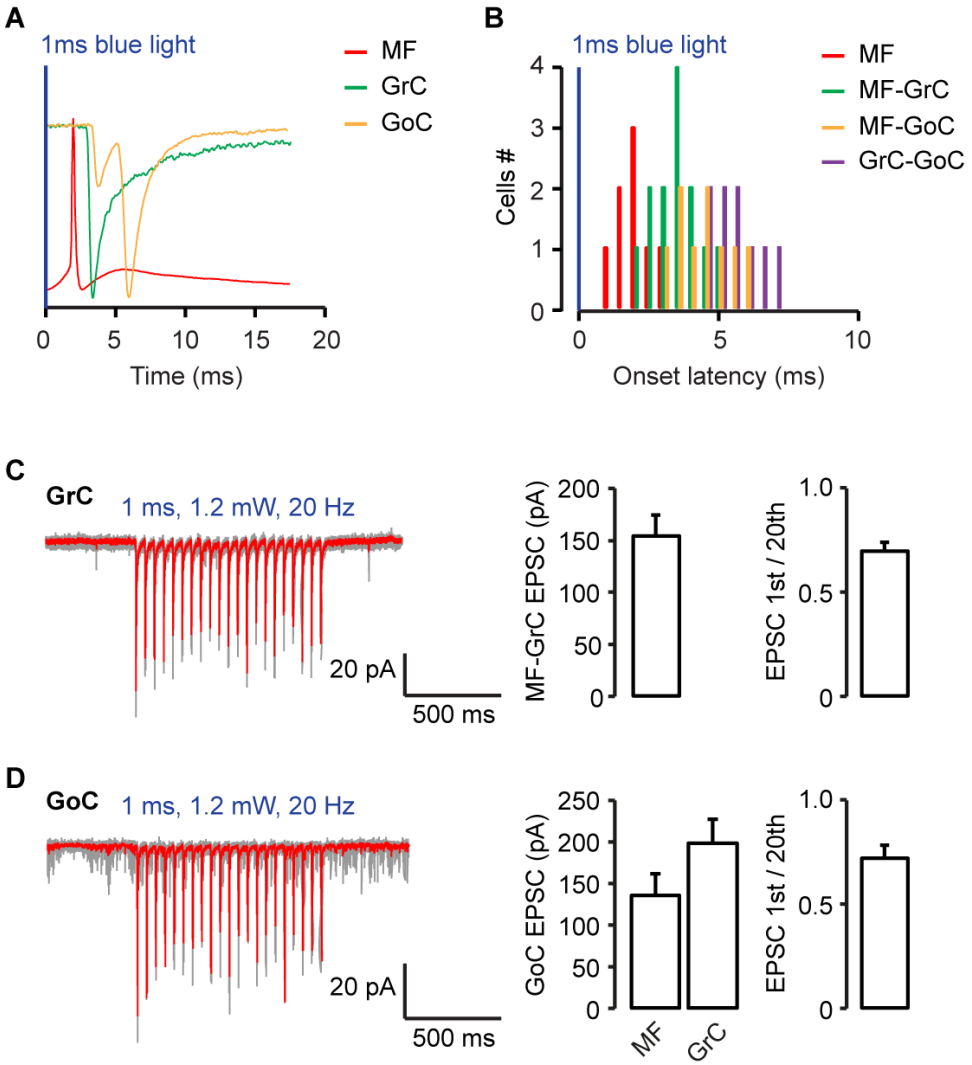

Figure S3. Related to Figure 4. Robust and sustained synaptic transmission between nucleocortical MF and cerebellar cortical neurons

(A) Monosynaptic delay between MF action potential and triggered EPSCs in GrC and GoC. Representative traces of triggered MF action potential, GrC EPSC and GoC EPSC. Traces are normalized for their amplitude and aligned to the start of light pulse. (B) Summary of the onset latency of the nucleocortical MF action potential (n = 10), MF-GrC EPSC (n = 13), MF-GoC and GrC-GoC EPSC (n = 9). (C) Sustained synaptic transmission from nucleocortical MF in response to repetitive stimulation. Left: 5 repetitive traces of MF-GrC EPSCs (gray) and the overlaying averaged trace (red) in response to an optogenetic train stimulation of 20 Hz. Right: summary of first EPSC amplitude and the ratio between the 1st and 20th EPSC during the train stimulation. (D) Similar to (C), left: MF-GoC EPSC in response to an optogenetic train stimulation of 20 Hz. Right: summary of first EPSC amplitude and the ratio between the 1st and 20th EPSC during the train stimulation.

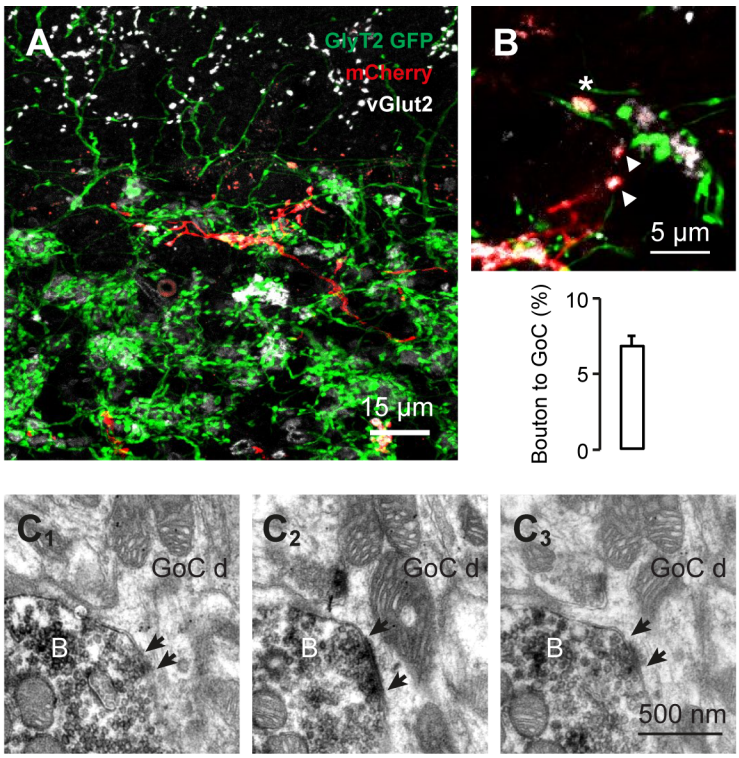

Figure S4. Related to Figure 6. Filopodial boutons form functional synapses with granule and Golgi cells.
(A) Representative image of a nucleocortical MF with filopodia protrusions in the cerebellum of GlyT2-eGFP mice. (B) Inset shows a vGlut2 positive filopodial bouton contacting a GlyT2-GFP positive Golgi cell dendrite (asterisk). Note that the surrounding boutons without contacting Golgi cell dendrites are indicated with arrowheads. Bar chart quantification shows the percentage of vGlut2 positive filopodial boutons that contact Golgi cell dendrites (21 MFs, N = 2). (C) Representative serial EM images of a BDA labeled filopodial bouton with synaptic contacts onto Golgi cell dendrites, as visualized with immunogold labeling. Arrows indicate synaptic contacts.

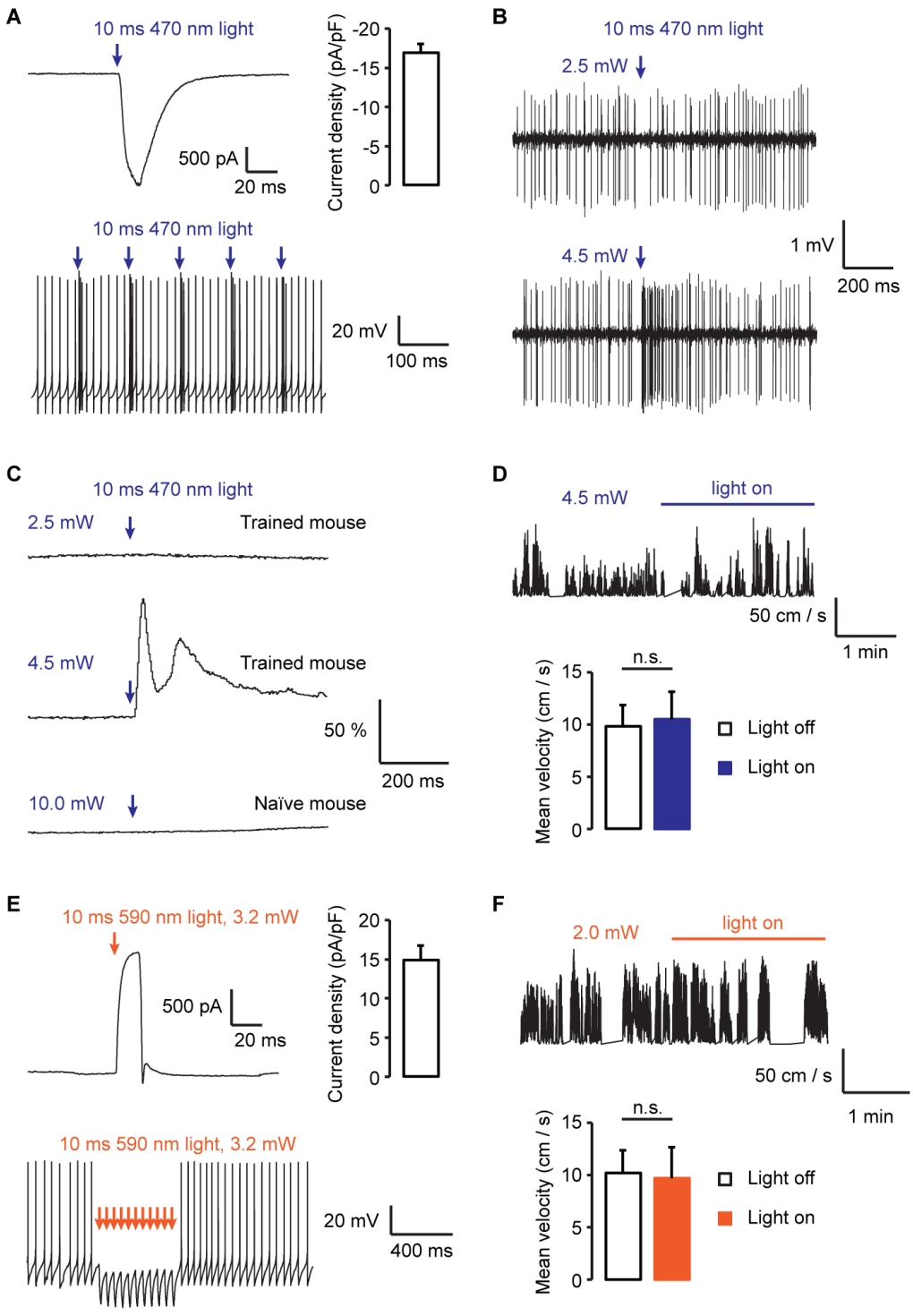

Figure S5. Related to Figure 8. Optogenetic control of nucleocortical activity and behavioral output

(A) Top left: photo current recorded from a ChR2 expressing CN neuron in response to a brief pulse of blue light. Top right: summary of photo current density in ChR2 expressing CN neurons (n = 4). Bottom: example traces showing that five light pulses reliably drive CN cell to fire extra action potentials. (B) Representative CN firing pattern *in vivo*. The optogenetic light intensity was gradually adjusted to probe the threshold for CN neuron direct activation (2.5 mW sub-threshold v.s. 4.5 mW

supra-threshold). For eyeblink conditioning experiments in Figure 8 light intensity was individually adjusted such that it did not exceed the CN activation threshold *in vivo*. (C) Optogenetic stimulation drives eyelid closure. 10 ms 4.5 mW but not 2.5 mW light stimulation directly drives eyelid closure in eyeblink conditioned mouse. Maximum light intensity did not induce detectable eyelid movement in naïve mice. (D) Prolonged subthreshold ChR2 optogenetic stimulation does not affect locomotion on the treadmill. Top: representative traces of running speed with/without optogenetic stimulation; bottom: summary of mean velocity (N = 6). (E) Top left: Photo current from an Arch3.0 expressing CN neuron in response to a brief pulse of amber light. Top right: summary of photo current density in Arch3.0 expressing CN neurons. Bottom: Five light pulses reliably drive CN cell to fire extra action potentials. Note the ChR2 in (A) and Arch3.0 expressing neurons in (E) show similar absolute current densities in our experiments. (F) Prolonged sub-threshold Arch3.0 optogenetic stimulation does not affect locomotion on the treadmill. Top: representative traces of running speed with/without optogenetic stimulation; bottom: summary of mean velocity (N = 5). Data show mean ± s.e., paired student's t-tests.

Supplemental Tables

Gao *et al*., Table S1

Mice	MF counted	MF per area (%)									
									Vermal lobules		
		Fl	PFl	PM	Cop	Crus 1	Crus 2	Sim	1-3	4-6	7-10
1	989	1.6	0.8	3.0	8.9	18.7	9.5	25.7	16.3	5.2	10.3
2	1037	1.0	0.0	0.9	7.2	12.1	3.9	25.8	27.1	17.9	4.1
3	1689	2.5	5.0	2.6	6.9	10.5	11.7	28.0	14.1	10.4	8.2
4	1100	1.2	2.5	3.0	8.9	12.1	15.2	34.2	6.1	12.0	4.9
5	1306	2.5	3.2	1.8	1.8	16.7	10.3	22.9	13.3	12.7	14.8
6	542	3.0	0.7	0.0	6.1	8.5	3.9	31.2	16.1	12.4	18.3
Mean		2.0	2.1	1.9	6.6	13.1	9.1	28.0	15.5	11.8	10.1
SD		0.8	1.9	1.2	2.6	3.9	4.5	4.1	6.8	4.1	5.6

Table S1. Related to Figure 1. Summary of nucleocortical mossy fiber distribution ipsilateral to the IpN injected with AAV vectors.
Fl: flocculus, PFl: paraflocculus, PM: paramedian lobule, Cop: copula pyramidis, Sim: lobule simplex.

Parameter	**NC + (n = 18)** Mean ± s.e.	**NC - (n = 14)** Mean ± s.e.	*t-tests*
Soma size (μm^2)	359.4 ± 45.2	382.7 ± 39.2	0.31
# Primary dendrites	4.2 ± 0.5	4.0 ± 0.3	0.60
Input resistance (MΩ)	145.5 ± 30.4	151.6 ± 25.9	0.47
AP threshold (mV)	-38.2 ± 1.0	-37.4 ± 1.2	0.62
AP amplitude (mV)	44.6 ± 0.8	44.4 ± 1.3	0.68
Rise time (ms)	1.0 ± 0.1	1.1 ± 0.1	0.56
Decay time constant (ms)	2.0 ± 0.8	2.2 ± 0.9	0.58
AP halfwidth (ms)	0.3 ± 0.01	0.3 ± 0.02	0.42
AHP (mV)	-12.5 ± 0.4	-13.3 ± 0.9	0.71

Table S2. Related to Figure 4. Comparisons of electrophysiological properties between identified nucleocortical projecting neurons (NC+) and large CN neurons without detectable nucleocortical axonal projection in the IpN (NC-).

Gao *et al*., Table S3

	Value	n		Value	n
Spontaneous firing rate (Hz)	39.5 ± 6.0	3	AP threshold (mV)	41.3 ± 1.5	7
Resting potential (mV)	-58.3 ± 3.8	7	AP amplitude (mV)	40.4 ± 5.2	7
Input resistance (MΩ)	387.3 ± 29.6	7	Rise time (ms)	0.3 ± 0.1	7
Capacitance (pF)	3.5 ± 1.4	7	Decay time constant (ms)	0.4 ± 0.1	7
Sag ratio	0.5 ± 0.06	7	AP halfwidth (ms)	0.3 ± 0.1	7
1st / 10th AP amplitude ratio	0.81 ± 0.1	7			

Table S3. Related to Figure 5. Summary of the electrophysiological properties of nucleocortical MF rosettes *in vitro*.

Supplemental Experimental Procedures

Animals. Male and female mice (C57BL/6) used for all the experiments were between 3 to 6 months of age and individually housed (food *ad libitum*, 12:12 light/dark cycle). All experimental protocols were approved by the institutional animal welfare committee (Erasmus MC, Rotterdam, The Netherlands).

Stereotaxic injections. Mice were anesthetized with a mixture of isoflurane/oxygen (5% for induction, 1.5-2.0% for maintenance). Rimadyl (5 mg/kg) and buprenorphine (0.05 mg/kg) were applied intraperitoneally 30 mins prior to surgery. Body temperature was monitored and kept constant at 37°C throughout the entire surgical procedure. A patch of skin above the skull was removed and local anesthetic (lidocaine) was topically applied. The skull was prepared with Optibond prime and adhesive (Kerr, Switzerland) and a pedestal was attached with Charisma (Heraeus Kulzer, NY, USA). Mice were then positioned on a custom-made mouse stereotaxic head-holding frame. Small craniotomies (0.2 mm) were made in corresponding sites and injections were performed using glass pipettes (tip opening between 5 and 10 µm) with mechanical pressure. For AAV injections, 60-120 nl of AAV2-hSyn-hChR2(H134R)-eYFP or AAV2-hSyn-eArch3.0-eYFP (10^{12}-10^{13} infectious units per ml, packaged by the UNC Joint Vector Laboratories, RRID: SCR_002448) were injected at a speed of 10 nl/min. For tracer injections, 20-100 nl Biotin Dextran Amine 10 kDa solution (10% w/v in saline, Life Technologies) and fluorescent Cholera toxin subunit-B (Ctb Alexa Fluor 488 and Ctb Alexa Fluor 555, 5% w/v in saline, Life Technologies) were injected at a speed of 10 nl/min. After each injection, the pipette was left in place for >10 minutes before being slowly withdrawn. Coordinates used for injections into the red nucleus were: 0.5 mm to Lambda, 0.5 mm lateral to midline and -4 mm ventral; for injections into the cerebellar lobule simplex: -2.0 mm to Lambda, 2.0 mm lateral to midline and -1.5 mm ventral; for injections into the interposed nucleus: -2.5 mm to Lambda, 2.5 mm lateral to midline and -2.3 mm ventral; for injections into the pontine nucleus: -0.5 mm to Lambda, 0.5 mm lateral to midline and -5.5 mm ventral. All mice were allowed to recover for >3 days before any subsequent procedure. Mice used for the optogenetic stimulations and extracellular recordings were subjected to additional surgery. 2-3 weeks after the virus injection (see above), under the same surgical conditions described above, an optic cannula (400 µm core, 0.39 NA, Thorlabs) was implanted into the lobule simplex with coordinates: -2.0 mm to Lambda, 2.0 mm lateral to midline and -0.5 to -1.0 mm ventral. A craniotomy (1.5 mm in diameter) was placed above Crus 1 and 2 to access the lobule simplex and the interposed nuclei. Antibiotic solution (Baytril 0.5%, Enrofloxacine 5 mg/ml) was applied topically after each experiment.

Eyeblink conditioning training. Head restrained mice were placed on top of a cylindrical treadmill and allowed to walk freely, see also (Heiney et al., 2014). We used a green LED placed 5-10 cm in front of the mouse as conditioned stimulus (CS). The duration of the CS for all the experiments was kept at 280 ms. The unconditional stimulus (US) consisted of an air-puff of 30 psi, 1 cm from the animal's cornea. The onset of the puff was 250 ms after the CS onset (inter-stimulus interval) and the duration was 30 ms, resulting in a co-termination of both stimuli. National Instruments NI-PXI (National Instruments, Austin TX, USA) processor was used to trigger and keep track of stimuli whilst capturing data. Eyelid position was illuminated by infrared LED light and recorded with a 250 fps camera (scA640-120gc, Basler, Ahrensburg, Germany) driven and acquired by custom written routines in LabVIEW. Mice were allowed to habituate on the treadmill for 2 days and followed by acquisition, in which 2 consecutive sessions were presented daily, each session consisting of 100 paired CS–US trials with inter-trial interval (ITI) 5-10 sec. The acquisition sessions were repeated for at least 5 consecutive days.

Optogenetics and electrophysiology *in vivo*. After the behavioral training and the placement of the optic cannula, we extracellularly recorded *in vivo* with or without optogenetic manipulation of the nucleocortical projecting fibers. For extracellular single-unit recordings, borosilicate glass pipettes (OD 1.5 mm, ID 0.86 mm, tip diameter 1-2 µm, Harvard Apparatus, Holliston, MA, USA) filled with 2 M NaCl were positioned stereotactically into the target regions using an electronic pipette micromanipulator (SM7; Luigs & Neumann, Ratingen, Germany). The behavioral responses and the neuronal activity were recorded in response to a brief pulse of light delivered to the brain via an optic fiber coupled with LED light sources (470 nm light for ChR2: M470F1; 590 nm light for eArch3.0 M590F1, Thorlabs). A brief pulse of 1-10 ms blue (470 nm) light or a 250 ms pulse of amber light (590 nm) was used to induce the activation or inhibition of nucleocortical mossy fibers. To avoid direct stimulation of CN soma, we only included data that met all the following criteria: 1) optic cannula were located in the superficial layer of the lobule simplex (see Figure 8A); 2) optogenetic

stimulation/inhibition was adjusted such that no instantaneous increase/decrease of action potential firing in the CN was observed; 3) optogenetic stimulation/inhibition did not result in instantaneous eyeblink responses; and 4) optogenetic stimulation/inhibition did not alter locomotion behavior (Figure S5). Locomotion was monitored using an incremental encoder coupled to the shaft of a cylindrical treadmill (EH30, Eltra, Italy). Purkinje cells were identified by the occurrence of simple spikes and complex spikes and were confirmed to be single unit by the occurrence of climbing fiber pause (Schonewille et al., 2010). Putative molecular layer interneurons were identified as previously described (Badura et al., 2013). CN neurons were identified by their stereotactic location and the characteristic neuronal activity (Hoebeek et al., 2010). Electrophysiological recordings were acquired with a Multiclamp 700B amplifier (Molecular Devices, Sunnyvale, USA) and band-pass filtered at 100-5,000 Hz. Electrophysiological and behavioral data were digitized synchronously using Digidata 1440A (Molecular Devices, Sunnyvale, USA) at 50 kHz. All *in vivo* data were analyzed using SpikeTrain software (Neurasmus BV, Rotterdam, The Netherlands) running under Matlab (Mathworks, MA, USA). Molecular layer interneurons and Purkinje cells were considered responsive if the post-optogenetic-activation firing frequency (measured <200 ms after the offset of light) exceeded 3 times standard deviation of the pre-optogenetic-activation frequency (measured 500 ms before the onset of light).

Optogenetics and electrophysiology *in vitro.* AAV injected mice were sacrificed >3 weeks post injection for *in vitro* experiments. Mice were decapitated under anaesthetized with isoflurane. 300 μm thick cerebellar coronal slices were cut on a vibratome (VT1200s, Leica, Wetzlar, Germany) in ice-cold slicing medium containing (in mM): 240 Sucrose, 5 KCl, 1.25 Na_2HPO_4, 2 $MgSO_4$, 1 $CaCl_2$, 26 $NaHCO_3$ and 10 D-Glucose, bubbled with 95% O_2 and 5% CO_2. Slices were incubated at 34°C for 1 h in the oxygenated ACSF containing (in mM): 124 NaCl, 2.5 KCl, 1.25 Na_2HPO_4, 1 $MgSO_4$, 2 $CaCl_2$, 26 $NaHCO_3$ and 25 D-Glucose and kept at room temperature (21 ± 1 °C) before use. All the experiments were performed with a constant flow of oxygenated ACSF (1.5-2.0 ml/min) at 34 ± 1 °C. Cerebellar neurons were visualized using an upright fluorescent microscope (Axioskop2 FS plus, Carl Zeiss, Jena, Germany) equipped with a 40X water immersion objective. A GFP filter was used to visualize the eYFP labeled mossy fiber terminals. Exposure time to epifuorescent light was kept short to prevent over activation of ChR2 with blue light. Acquired fluorescent images were digitally aligned with the DIC images for identifying eYFP positive mossy fiber rosettes. Whole cell and cell attached patch-clamp recordings of nucleocortical mossy fiber rosettes, granule cells, Golgi cells, Purkinje cells, and cerebellar nuclei neurons were performed under DIC visualization. Patch-clamp recordings were performed using an EPC-10 double amplifier controlled by the Patchmaster software (HEKA electronics, Lambrecht, Germany). All recordings were low-pass filtered at 5 kHz and digitized at 20 kHz. Borosilicate glass pipettes (WPI) were filled with intracellular solution containing the following (in mM): 120 K-gluconate, 9 KCl, 10 KOH, 3.48 $MgCl_2$, 4 NaCl, 10 HEPES, 4 Na_2ATP, 0.4 Na_3GTP and 17.5 sucrose (pH 7.25) and had pipette resistances of 8-10 MΩ for recording mossy fiber rosettes, 4-6 MΩ for recording granule cells and Golgi cells, and 3-4 MΩ for recording Purkinje cells and cerebellar nuclei neurons. Optogenetic stimulation was delivered via the epifluorescent light path. The light intensity was adjusted to 0.1 - 4 mW/mm^2. The light path was controlled by a mechanical shutter (LS2, Vincent Associates, USA). The shutter opening jitter was measured to be 3 ms and was subtracted from all the onset times of the EPSCs driven by optogenetic manipulation. EPSCs in granule and Golgi cells were recorded by holding cells at -70 mV in voltage-clamp mode. Action potential firing was recorded in current-clamp mode without holding current (I = 0). For comparing the inhibition/excitation (I/E) ratios following optogenetic activation of nucleocortical MFs afferents with that of the local electrical activation of a mixed group of MFs, we chose only the Purkinje cells in the lobule simplex that showed clear optogenetically induced EPSCs. For electrical stimulation, a second electrode connected with an Iso-Flex stimulus isolator (A.M.P.I., Jerusalem, Israel) was placed in the white matter adjacent to the recorded Purkinje cells. EPSC and IPSC components were isolated with intracellular solution containing: 120 Cs-gluconate, 10 CsOH, 3.48 $MgCl_2$, 4 NaCl, 10 HEPES, 4 Na_2ATP, 0.4 Na_3GTP and 17.5 sucrose (pH 7.25). EPSCs were acquired at -75 mV, close to the reversal potential of GABAA receptors. The electrical stimulation intensity was adjusted so that the EPSC amplitude was comparable to that of the optogenetic stimulation. The IPSC components were subsequently recorded with holding potential of 0 mV, close to the reversal potential of AMPA receptors. The ratio of the positive peak amplitude at 0 mV and negative peak amplitude at -75 mV was taken as a function of the I/E ratio. To compare the electrophysiological properties of cerebellar neurons between naïve and trained mice, we repeated similar patch clamp recordings in granule cells and Purkinje cells in a group of mice that were fully trained with the eyeblink conditioning paradigm (see eyeblink conditioning section).

Immunohistochemistry and analysis. Mice were deeply anesthetized with an overdose of Nembutal (i.p.) and transcardially perfused with 20 ml saline followed by 50 ml 4% PFA. Brains were extracted and post-fixed overnight in 4% PFA at 4°C. Brains were subsequently embedded in gelatine and cryoprotected in 30% sucrose in PB, frozen on dry ice, and sectioned using a freezing microtome (40 µm thick). For light microscopy analysis of the mice injected with BDA, free-floating sections were blocked for 1h at room temperature in 10% NHS PB solution with 1% triton and visualized with the avidin-biotin-peroxidase complex method (ABC) (Vector Laboratories, Burlingame, USA,) and diaminobenzidine (DAB, 0.05%, Life Technologies) as the chromogen. For immunofluorescent staining, free-floating sections were blocked for 1 h at room temperature in PBS with 0.4% Triton X-100 and 10% NHS solution and incubation 48 hrs at 4°C in a mixture of primary antibodies diluted in PBS with 2% NHS and 0.4% Triton X-100. Sections were then washed and incubated for 2 h at room temperature in a mixture of fluorescent secondary antibodies. Primary antibodies used were rabbit anti-VGlut1 (1:1000, Synaptic Systems, RRID: AB_887876), guinea pig anti-VGlut2 (1:1000, Millipore, RRID: AB_1587626), mouse anti-Calbindin D28K (1:7000, Sigma, RRID: AB_2313712), and goat anti-*Zebrin II* (1:1000, Santa Cruz, RRID: AB_2226594). Slices were then counterstained with DAPI (1:100,000, Invitrogen) and mounted with mounting medium for fluorescence (Vectashield H-1000). All images were acquired on an upright LSM 700 confocal microscope (Carl Zeiss, Jena, Germany) and post-hoc adjusted and analyzed in FIJI software with appropriate plugins (http://pacific.mpi-cbg.de). Ctb labeled neurons were recognized as 'web-like' Golgi apparatus labeling surrounding DAPI labeled cell nuclei, distinct from bouton-like labeling of Purkinje cell axon terminals (Fig. 1). For visualization of the granule and Golgi cell morphology after *in vitro* electrophysiological recordings, Alexa Fluor 555 or 594 (20 µM, Life Technologies) were added to the intracellular solution. For detailed quantification of CN neuron morphology, biocytin (1% w/v) was added to the intracellular solution and visualized with streptavidin Alexa Fluor 488 (1:400, Life Technologies). Immediately after recording, cerebellar slices were fixated in 4% PFA at room temperature for 2-5 hrs, washed in PBS and mounted with mounting medium for fluorescence (Vectashield H-1000). To prevent shrinkage and distortion of thick sections, special care was taken during mounting processes. Cell morphology was acquired on an upright LSM 700 confocal microscope (Carl Zeiss, Jena, Germany) and quantified with FIJI and Neurolucida (MBF bioscience, Williston, USA) software. Nucleocortical projecting IpN neurons were defined following reconstruction of the cell body and axonal projection (see Figure 5). We consider that potential non-nucleocortical projecting neurons are the neurons of which both dendritic tree and axonal projection towards cerebellar peduncle appeared complete, yet no cortical projection was observed.

Immuno-electron microscopy. BDA injected mice were anesthetized with an overdose of nembutal (i.p.) and transcardially perfused with 10 ml saline and subsequently 50 ml 4% PFA and 0.5% glutaraldehyde in cacodylate buffer. Cerebellum was removed and post-fixed overnight in 4% PFA. 80-µm thick coronal sections were cut on a vibratome (Technical Products International, St. Louis, USA). BDA labeled MF rosettes were visualized by incubating the sections with the avidin-biotin-peroxidase complex method (ABC) for 24-48 hrs (Vector Laboratories, USA) and subsequently developed with DAB (0.05%, Life Technologies) as the chromogen. The vibratome sections were rinsed and post-fixed in 1% osmium tetroxide, stained with 1% uranyl acetate, dehydrated and embedded in araldite (Durcupan ACM; Fluka, Buchs, Switzerland). Ultrathin (50-70 nm) sections were cut on an ultramicrotome (Leica, Wetzlar, Germany), mounted on formvar-coated copper grids and contrasted with 2% uranyl acetate and 1% lead citrate (Fluka). For postGABA immunocytochemistry, the grids were rinsed in 0.5 M of Tris buffer with 0.9% NaCl and 0.1% Triton X-100, pH 7.6 (TBST), and incubated overnight at 4ºC in (Sigma, 1:1500 in TBST). The grids were subsequently rinsed twice with TBST and incubated for 1 h at room temperature in goat anti-rabbit IgG labeled with 10 nm gold particles (Aurion) diluted 1:25 in TBST. Cerebellar sections containing BDA positive MFs were photographed using an electron microscope (Philips, Eindhoven, Netherlands). Electron micrographs were analyzed using FIJI software.

Statistical methods. Values are represented as mean ± s.e.; p values of <0.05 were considered significant and are reported in the main text. Statistical analysis was done using student's t-test, unless stated otherwise.

Supplemental References

Badura, A., Schonewille, M., Voges, K., Galliano, E., Renier, N., Gao, Z., Witter, L., Hoebeek, F.E., Chedotal, A., and De Zeeuw, C.I. (2013). Climbing fiber input shapes reciprocity of Purkinje cell firing. Neuron 78, 700-713.

Heiney, S.A., Wohl, M.P., Chettih, S.N., Ruffolo, L.I., and Medina, J.F. (2014). Cerebellar-dependent expression of motor learning during eyeblink conditioning in head-fixed mice. The Journal of neuroscience : the official journal of the Society for Neuroscience 34, 14845-14853.

Hoebeek, F.E., Witter, L., Ruigrok, T.J., and De Zeeuw, C.I. (2010). Differential olivo-cerebellar cortical control of rebound activity in the cerebellar nuclei. Proceedings of the National Academy of Sciences of the United States of America 107, 8410-8415.

Schonewille, M., Belmeguenai, A., Koekkoek, S.K., Houtman, S.H., Boele, H.J., van Beugen, B.J., Gao, Z., Badura, A., Ohtsuki, G., Amerika, W.E*., et al.* (2010). Purkinje cell-specific knockout of the protein phosphatase PP2B impairs potentiation and cerebellar motor learning. Neuron 67, 618-628.